



Magnetic properties of A- and B-site cation doped $\text{La}_{0.65}\text{Ca}_{0.35}\text{MnO}_3$ manganites

Y. Samancıoğlu, A. Coşkun*

Department of Physics, Faculty of Sciences and Letters, Mugla University, TR-48000, Kötekli, Muğla, Turkey

ARTICLE INFO

Article history:

Received 19 July 2010

Received in revised form 28 July 2010

Accepted 30 July 2010

Available online 4 August 2010

Keywords:

Composite materials

Sol–gel processes

Magnetocaloric effect

Magnetic measurements

ABSTRACT

The $\text{La}_{0.65}\text{Ca}_{0.35}\text{MnO}_3$, $\text{La}_{0.65}\text{Ca}_{0.30}\text{Pb}_{0.05}\text{MnO}_3$ and $\text{La}_{0.65}\text{Ca}_{0.30}\text{Pb}_{0.05}\text{Mn}_{0.9}\text{Cu}_{0.1}\text{O}_3$ compounds, prepared by the sol–gel method and sintered in air at 1100°C for 24 h, have been investigated by Magnetic Properties Measurements System (MPMS) to explore the effects of A- and B-site cation doping. From the measurements, the Curie temperatures (T_C) and the isothermal magnetic entropy changes ($-\Delta S_M$) were determined. The Curie temperature of $\text{La}_{0.65}\text{Ca}_{0.35}\text{MnO}_3$ compound was found to be 273 K. The Curie temperature increases to 286 K for the $\text{La}_{0.65}\text{Ca}_{0.30}\text{Pb}_{0.05}\text{MnO}_3$ compound due to the substitution of Ca by a small amount of Pb. However, replacing 10% of Mn with Cu ($\text{La}_{0.65}\text{Ca}_{0.30}\text{Pb}_{0.05}\text{Mn}_{0.9}\text{Cu}_{0.1}\text{O}_3$) leads to a reduction in the Curie temperature to 223 K. For the field change of 1 T, while the maximum magnetic entropy change for the sample $\text{La}_{0.65}\text{Ca}_{0.35}\text{MnO}_3$ was found to be 4.1 J/kg K it decreases down to 2.6 J/kg K and 3.2 J/kg K for the $\text{La}_{0.65}\text{Ca}_{0.30}\text{Pb}_{0.05}\text{MnO}_3$ and $\text{La}_{0.65}\text{Ca}_{0.30}\text{Pb}_{0.05}\text{Mn}_{0.9}\text{Cu}_{0.1}\text{O}_3$ samples, respectively.

© 2010 Elsevier B.V. All rights reserved.

1. Introduction

Cooling systems, seen in all areas of daily life, are widely used for keeping our foods cool and living spaces at comfort temperatures. Today, process of cooling is mostly realized by means of vapor compression. For very low temperature ($<10\text{K}$) magnetic cooling systems, based on magnetizing and demagnetizing a paramagnetic material, are becoming to be preferential and widespread. Although the magnetocaloric effect (MCE) has been known for years, significant studies in this field have been carried out during the last couple decades [1–5]. The discovery, that Gd and some of its alloys exhibit large MCE, has triggered intensive studies on these materials [6–9]. Besides, recent studies have also shown that manganite compounds in the chemical form of $\text{La}_{1-x}\text{A}_x\text{MnO}_3$ where (A is a monovalent ion such as Na, Li, Ag and K or a divalent ion such as Ca, Sr, Ba and Pb) exhibit large MCE around room temperature [10–13]. It is often expressed that these manganite based compounds have an important potential for the development of magnetic cooling systems in commercial means, because the intrinsic negations seen in Gd and in the other rare earth elements do not show up in these compounds. Additionally, the low production costs, the ease of shaping and preparation and low magnetic hysteresis are among the other superiorities of these materials. Yet, the needed optimization of all parameters in order for these materials to be used as active magnetic cooling element for room temperature applications has not been accomplished.

From the research papers on the effect of monovalent or divalent ion doping of these compounds in La site (A-site) on the magnetic properties it is seen that some magnetic properties are affected positively; some negatively [14–16]. It is known that the magnetic properties of these compounds are very sensitive to the average valence state of the Mn ions, since the electronic configuration and average ionic radius of the manganese site (B-site) depend on the average valence state of the Mn ions. If the substituted ion (A in $\text{La}_{1-x}\text{A}_x\text{MnO}_3$) is divalent, it oxidizes a Mn^{3+} ion to Mn^{4+} ion, but if it is a monovalent ion, it oxidizes two Mn^{3+} ions to two Mn^{4+} ions. Therefore, $\text{Mn}^{3+}/\text{Mn}^{4+}$ ratio changes, depending on the valence state and the concentration of the substitute ion. Mn^{3+} and Mn^{4+} ions differ in their ionic radii. La^{3+} and the substitute ion in A-site may also have different ionic radii. Because of these ionic radii differences, the concentration level plays very important role in the formation of crystal structure of the resulting compounds as well as in magnetic properties. In this work, 0.35 Ca and 0.30 Ca + 0.05 Pb have been chosen for the doping in the A-site. Both Ca and Pb ions have 2+ valence state and with the concentration levels given above, $\text{Mn}^{3+}/\text{Mn}^{4+}$ ratio is made fixed, in order to explore the effect of the average ionic radius, $\langle r_A \rangle$, of the A-site. In addition to the A-site doping, it is possible to simultaneously dope the B-site of these compounds. Some transition metals (Fe, Cu, Ni, Co, etc.) have been used as doping element in the B-site [17–19]. Cu doping in the B-site has been done in this study because of both the double valuedness of the valence state of Cu ions and differences of its ionic radius in case of 2+ and 3+ valence states. The results in the literature related to the valence state of Cu ions within the structure of B-site doped compounds are diverse.

O. Klyushnikov et al., claim that the oxidation state of Cu is 2+ in the $\text{La}_{0.70}\text{Ca}_{0.30}\text{Mn}_{0.97}\text{Cu}_{0.03}\text{O}_3$ compound, based on their X-

* Corresponding author. Tel.: +90 252 211 1586.

E-mail address: coskunatilla@gmail.com (A. Coşkun).

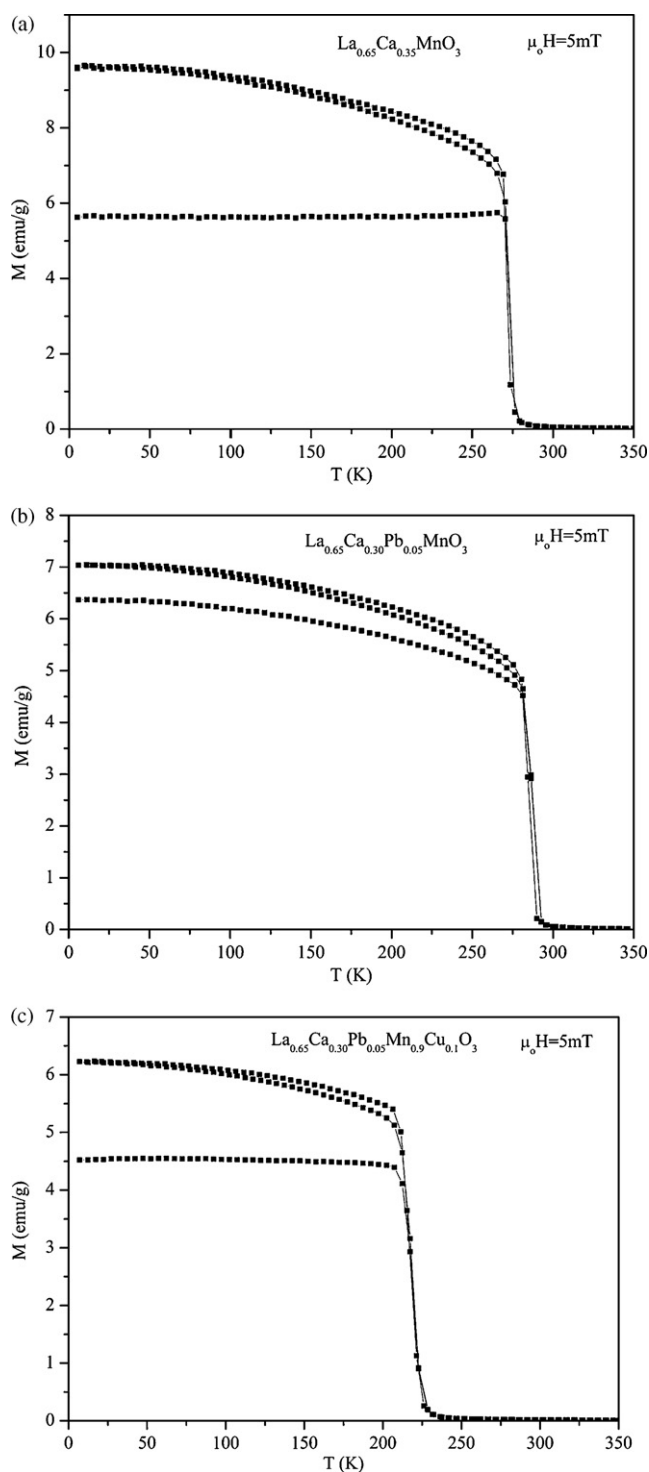


Fig. 1. Temperature dependence of the magnetization at $\mu_0 H = 50$ mT for the samples: (a) $\text{La}_{0.65}\text{Ca}_{0.35}\text{MnO}_3$, (b) $\text{La}_{0.65}\text{Ca}_{0.30}\text{Pb}_{0.05}\text{MnO}_3$, (c) $\text{La}_{0.65}\text{Ca}_{0.30}\text{Pb}_{0.05}\text{Mn}_{0.90}\text{Cu}_{0.10}\text{O}_3$.

ray photoelectron spectroscopy (XPS) results [20]. Pi et al. have investigated the magnetic properties of $\text{La}_{0.825}\text{Sr}_{0.175}\text{Mn}_{1-x}\text{Cu}_x\text{O}_3$ ($0 < x < 0.20$) compounds. They concluded that the strength of ferromagnetism of their samples decreases with the increase of Cu content. They claim that the valence state of Cu ions is 2+, hence, Cu substitution increases the content of the Mn^{4+} ions and antiferromagnetic superexchange interaction becomes dominant. At the same time, the $\text{Mn}^{3+}-\text{O}^{2-}-\text{Mn}^{4+}$ bonds are destroyed gradually [21]. Zhou et al. have investigated the transport and magnetic

Table 1

The values of the $\langle r_A \rangle$, $\langle r_B \rangle$, T_C , $\text{Mn}^{3+}/\text{Mn}^{4+}$ ratio for the $\text{La}_{0.65}\text{Ca}_{0.35}\text{MnO}_3$, $\text{La}_{0.65}\text{Ca}_{0.30}\text{Pb}_{0.05}\text{MnO}_3$ and $\text{La}_{0.65}\text{Ca}_{0.30}\text{Pb}_{0.05}\text{Mn}_{0.90}\text{Cu}_{0.10}\text{O}_3$.

Compound	$\langle r_A \rangle$ (Å)	$\langle r_B \rangle$ (Å)	T_C (K)	$\text{Mn}^{3+}/\text{Mn}^{4+}$
$\text{La}_{0.65}\text{Ca}_{0.35}\text{MnO}_3$	1.2034	0.6047	273	1.857
$\text{La}_{0.65}\text{Ca}_{0.30}\text{Pb}_{0.05}\text{MnO}_3$	1.2109	0.6047	286	1.857
$\text{La}_{0.65}\text{Ca}_{0.30}\text{Pb}_{0.05}\text{Mn}_{0.90}\text{Cu}_{0.10}^{2+}\text{O}_3$	1.2109	0.6017	223	1.000
$\text{La}_{0.65}\text{Ca}_{0.30}\text{Pb}_{0.05}\text{Mn}_{0.90}\text{Cu}_{0.10}^{3+}\text{O}_3$	1.2109	0.5942	223	1.571

properties of $\text{La}_{0.7}\text{Ca}_{0.3}\text{Mn}_{1-x}\text{Cu}_x\text{O}_3$ compounds. They have found shifting in the T_C values towards lower temperatures and broadening in the width of the magnetic transition region with increasing Cu content. They also observed, through XPS analysis, that some of Cu ions entering into sample is in the form of Cu^{3+} , besides Cu^{2+} [22].

The purpose of this work is to investigate the effect of Pb substitution in A-site and Cu substitution in B-site on the magnetic and magnetocaloric properties of $\text{La}_{0.65}\text{Ca}_{0.35}\text{MnO}_3$ compound. It is expected that the substitution of an element having different ionic radii and valence state causes variations in the average ionic radius of both A and B-sites ($\langle r_A \rangle$, $\langle r_B \rangle$). Depending on these variations, Mn–O bond length and Mn–O–Mn bond angle change and ferromagnetic double exchange interaction and antiferromagnetic superexchange interaction between the neighboring Mn ions also change. These changes alter the behavior of the magnetic phase transition of the compounds. So, different element substitution in the parent compound will influence magnetic properties. Further, depending on differences in ionic radii of Mn^{3+} and Mn^{4+} ions, if any change occurs in the number of these two ions, it will directly change the $\text{Mn}^{3+}/\text{Mn}^{4+}$ ratio and $\langle r_B \rangle$, and hence change the magnetic properties of the compounds.

2. Experimental

In this study, the $\text{La}_{0.65}\text{Ca}_{0.35}\text{MnO}_3$, $\text{La}_{0.65}(\text{Ca}_{0.30}\text{Pb}_{0.05})\text{MnO}_3$ and $\text{La}_{0.65}(\text{Ca}_{0.30}\text{Pb}_{0.05})\text{Mn}_{0.90}\text{Cu}_{0.10}\text{O}_3$ samples have been prepared by the sol-gel method. For each compound, appropriate amounts of La_2O_3 , CaCO_3 , $\text{Pb}(\text{NO}_3)_2$, $\text{Mn}(\text{NO}_3)_2$ and CuO were dissolved in dilute HNO_3 solution at 150°C . Then citric acid and ethylene glycol were added to the mixture. Viscous residual was formed by slowly boiling this solution at 200°C . The obtained residual was dried slowly at 300°C until dry-gel was formed. Finally, the residual precursor was burned in air at 600°C in order to remove organic materials produced during chemical reactions. The material obtained from this process was ground to fine powder by using an agate mortar. Three pellets of 13 mm diameter and 2 mm thickness were produced by pressing under the pressure of 3 tons. Each pellet was then sintered at 1100°C for 24 h in air and cooled down to room temperature in the furnace.

The magnetic properties were measured by using a Quantum Design MPMS in the temperature range 5–300 K with magnetic fields up to 5 T. From the temperature dependence of magnetization, T_C values were determined in an applied field of 50 Oe. In the zero-field-cooled (ZFC) measurement sequence, the sample is first cooled down to 5 K under zero-field and then, the field of 50 Oe is applied, and the magnetization of the sample is measured up to 300 K. Subsequently, without removing the field, the magnetization is measured down to 5 K (field cooled: FC). In order to determine the magnetocaloric properties, magnetization versus magnetic field $M(H)$ measurements were made on increasing fields between 0 and 5 T, at constant temperatures around T_C in steps of 3 K.

3. Results and discussions

In Fig. 1a–c the temperature dependence of magnetizations, $M(T)$, under both zero field and field cooling conditions, employing an applied field of 50 Oe are shown. The Curie temperature, T_C , was found to be 273 K for the $\text{La}_{0.65}\text{Ca}_{0.35}\text{MnO}_3$ sample. This T_C value is higher than the most of the values reported in the literature. Koubaa et al. obtained 248 K for the same compound which was prepared by the solid-state reaction method and sintered at 1100°C [23]. Zhang et al. found the magnetic transition temperature to be 267.9 K, for $\text{La}_{0.65}\text{Ca}_{0.35}\text{MnO}_3$; about 5 K lower than value observed in this work. Like us they also utilized the sol-gel method for the sample preparation and sintered the sample at 1200°C [24].

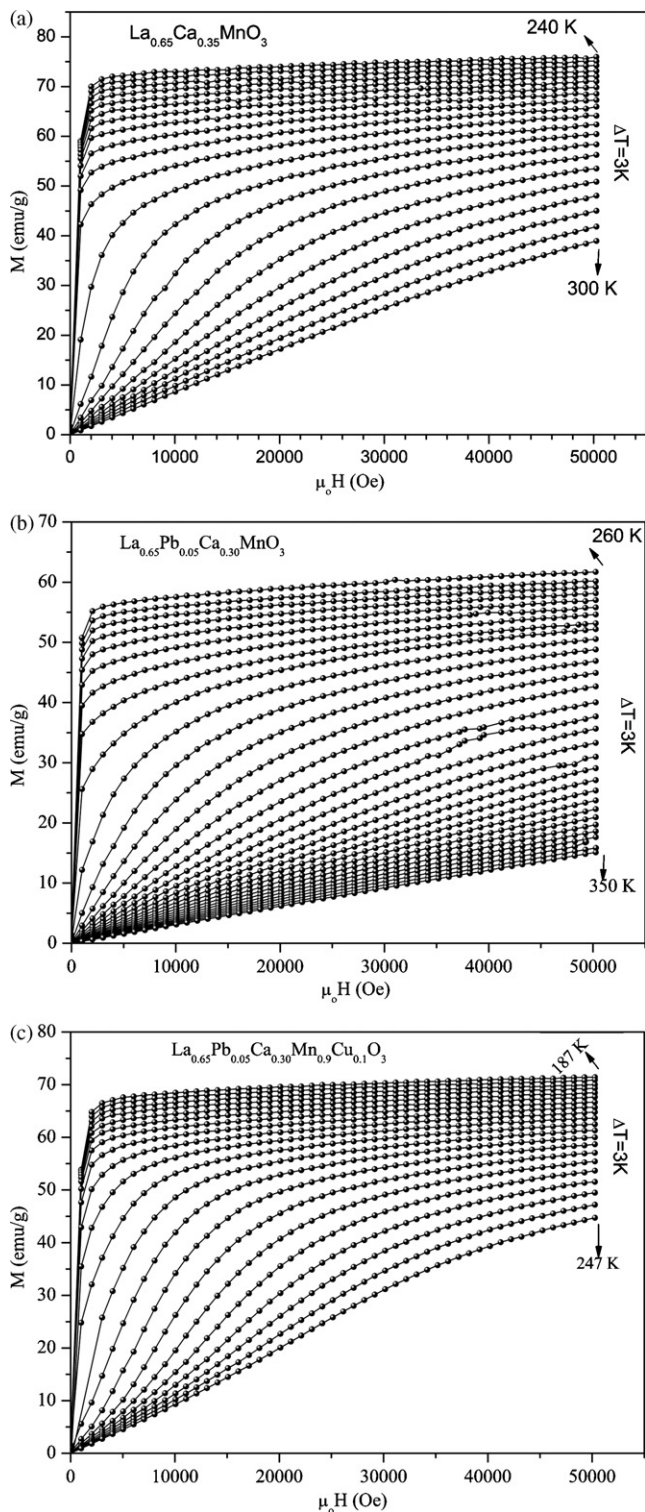


Fig. 2. Magnetization versus applied magnetic field μ_0H at different temperatures for the samples: (a) $\text{La}_{0.65}\text{Ca}_{0.35}\text{MnO}_3$, (b) $\text{La}_{0.65}\text{Ca}_{0.30}\text{Pb}_{0.05}\text{MnO}_3$, (c) $\text{La}_{0.65}\text{Ca}_{0.30}\text{Pb}_{0.05}\text{Mn}_{0.90}\text{Cu}_{0.10}\text{O}_3$.

It is well known that there are several factors affecting the paramagnetic to ferromagnetic phase transition temperature in the doped $\text{A}_{1-x}\text{B}_x\text{O}_3$ type manganite compounds. One of them is the average A-site ionic radius, $\langle r_A \rangle$, changing with the ionic radius of the substituted ion and its concentration. The average ionic radius of A-site has an impact on the lattice parameters of the perovskite structure. Therefore, the Mn–O bond length and Mn–O–Mn

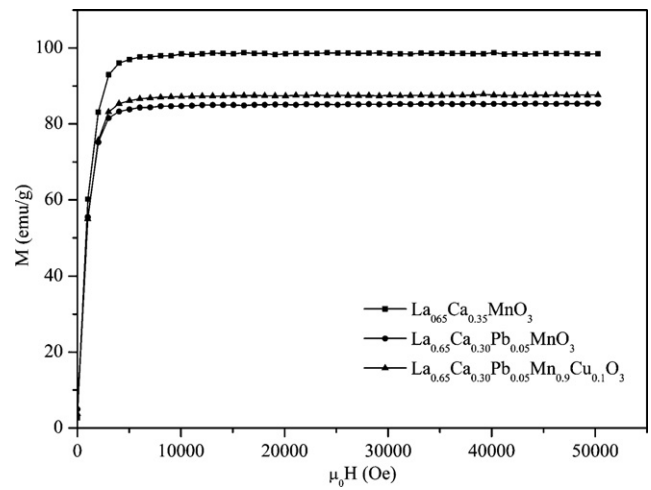


Fig. 3. Variation of the magnetization versus the applied magnetic field μ_0H measured at temperature of 5 K for the samples $\text{La}_{0.65}\text{Ca}_{0.35}\text{MnO}_3$, $\text{La}_{0.65}\text{Ca}_{0.30}\text{Pb}_{0.05}\text{MnO}_3$ and $\text{La}_{0.65}\text{Ca}_{0.30}\text{Pb}_{0.05}\text{Mn}_{0.90}\text{Cu}_{0.10}\text{O}_3$.

bond angle may change according to the ionic radius of the substituted ion and its concentration. Another important factor is the strong electron-phonon coupling due to the Jahn-Teller distortion of the MnO_6 octahedra [25]. When small amount of Ca^{2+} ions was replaced by Pb^{2+} ions in the A-site the T_C value was increased, i.e., the T_C has been found to be 286 K for the $\text{La}_{0.65}\text{Ca}_{0.3}\text{Pb}_{0.05}\text{MnO}_3$ sample. Although, the $\text{Mn}^{3+}/\text{Mn}^{4+}$ ratio remains the same for the Pb added sample as for the parent compound, the T_C increases due to the increase in the average A-site ionic radius (r_A) (see Table 1). The larger ionic radius of Pb (1.33 Å) compared to Ca (1.18 Å) leads to alterations in Mn–O bond length and Mn–O–Mn bond angle. As a result, it changes the traveling path of e_g electrons hopping between Mn ions, in turn, affecting the strength of the magnetic coupling between neighboring Mn ions.

The A-site cation size mismatch is defined as $\sigma^2 = \sum_i y_i r_i^2 - \langle r_A \rangle^2$, where y_i represents the concentration of the entities constituting the A-site, r_i is the radius of each one. The calculated σ^2 values are $0.000295(\text{\AA})^2$ and $0.001013(\text{\AA})^2$ for the $\text{La}_{0.65}\text{Ca}_{0.35}\text{MnO}_3$ and $\text{La}_{0.65}\text{Ca}_{0.3}\text{Pb}_{0.05}\text{MnO}_3$ samples, respectively. This large variation in σ^2 for the $\text{La}_{0.65}\text{Ca}_{0.3}\text{Pb}_{0.05}\text{MnO}_3$ sample arises from the replacement of small Ca^{2+} ions by large Pb^{2+} ions. The size mismatch causes a local distortion of MnO_6 octahedra. There are large lattice distortions in the neighborhood of Pb ions which cause a local shift in the Mn–O–Mn bond angle and Mn–O length. It is possible that the local lattice distortion with large value of σ^2 for the $\text{La}_{0.65}\text{Ca}_{0.3}\text{Pb}_{0.05}\text{MnO}_3$ sample tends to provide suitable pathway for the e_g electrons hopping between Mn^{3+} and Mn^{4+} ions and enhances long-range ferromagnetic order leading to an increase in the T_C value.

The magnetic phase transition temperature of the B-site doped $\text{La}_{0.65}\text{Ca}_{0.30}\text{Pb}_{0.05}\text{Mn}_{0.90}\text{Cu}_{0.10}\text{O}_3$ compound was measured to be 223 K. It is possible to speculate that the decrease in T_C stems from the change in the $\text{Mn}^{3+}/\text{Mn}^{4+}$ ratio due to the Cu ions being involved in the structure. Because of the existence of Cu ions within the structure, the number of the Mn^{4+} ions increases, which favors antiferromagnetic $\text{Mn}^{4+}\text{--O--Mn}^{4+}$ superexchange interactions. Meanwhile, the ferromagnetic $\text{Mn}^{3+}\text{--O--Mn}^{4+}$ hopping interactions decrease.

The variations in $\langle r_A \rangle$, $\langle r_B \rangle$, T_C and the $\text{Mn}^{3+}/\text{Mn}^{4+}$ ratio of the compounds are given in Table 1. In the calculation of these parameters, possible valence states of Cu ions (Cu^{2+} or Cu^{3+}) were taken into consideration for the $\text{La}_{0.65}\text{Ca}_{0.30}\text{Pb}_{0.05}\text{Mn}_{0.90}\text{Cu}_{0.10}\text{O}_3$ sample. Although, the $\text{Mn}^{3+}/\text{Mn}^{4+}$ ratios are the same for the $\text{La}_{0.65}\text{Ca}_{0.35}\text{MnO}_3$ and the $\text{La}_{0.65}\text{Ca}_{0.3}\text{Pb}_{0.05}\text{MnO}_3$ samples, their A-

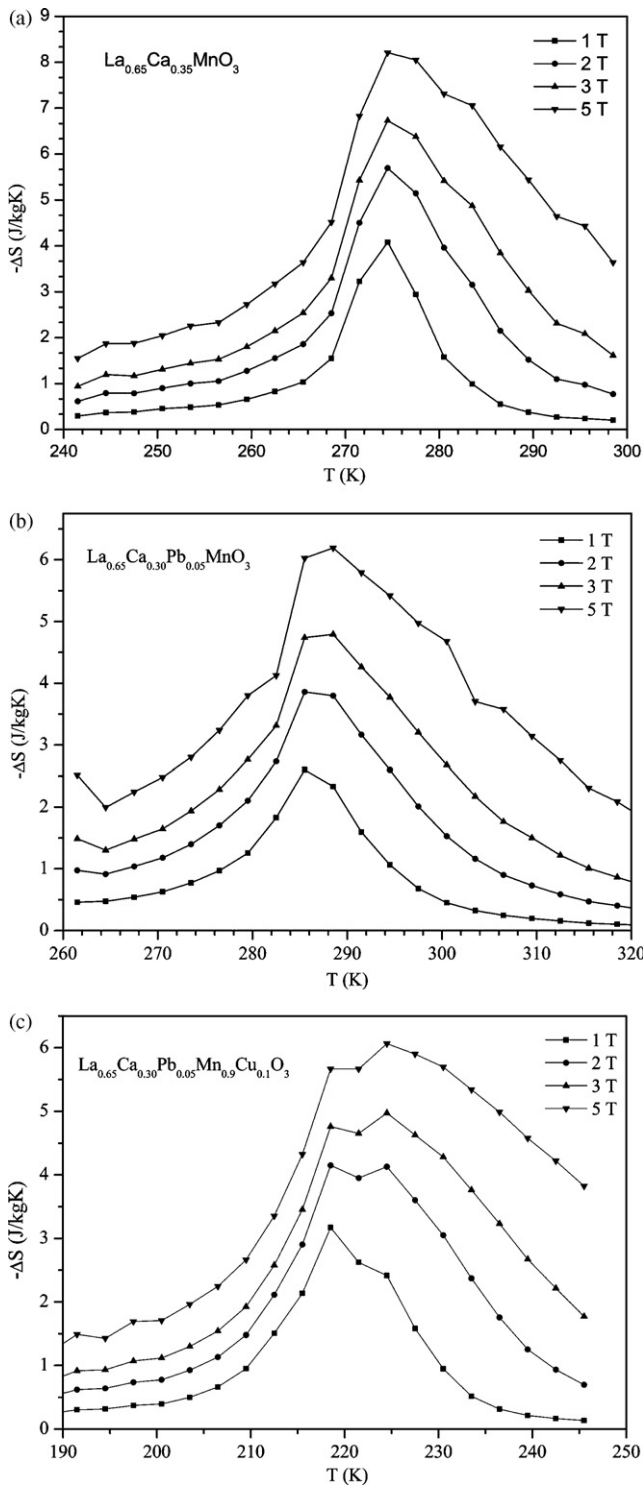


Fig. 4. Temperature dependence of the magnetic entropy change at several magnetic applied field for the samples: (a) $\text{La}_{0.65}\text{Ca}_{0.35}\text{MnO}_3$, (b) $\text{La}_{0.65}\text{Ca}_{0.30}\text{Pb}_{0.05}\text{MnO}_3$, (c) $\text{La}_{0.65}\text{Ca}_{0.30}\text{Pb}_{0.05}\text{Mn}_{0.90}\text{Cu}_{0.10}\text{O}_3$.

site average ionic radii (r_A) are different. This may be the reason that the T_C value of the $\text{La}_{0.65}\text{Ca}_{0.30}\text{Pb}_{0.05}\text{MnO}_3$ sample is higher than that of the $\text{La}_{0.65}\text{Ca}_{0.35}\text{MnO}_3$ sample. The increase in (r_A) due to the larger ionic radius of the Pb ions is an important factor influencing the magnetic properties of the $\text{La}_{0.65}\text{Ca}_{0.30}\text{Pb}_{0.05}\text{MnO}_3$ compound.

For the $\text{La}_{0.65}\text{Ca}_{0.30}\text{Pb}_{0.05}\text{Mn}_{0.90}\text{Cu}_{0.10}\text{O}_3$ sample we have to take some conditions into consideration. When the oxidation state of the Cu ions in the structure is 2+,

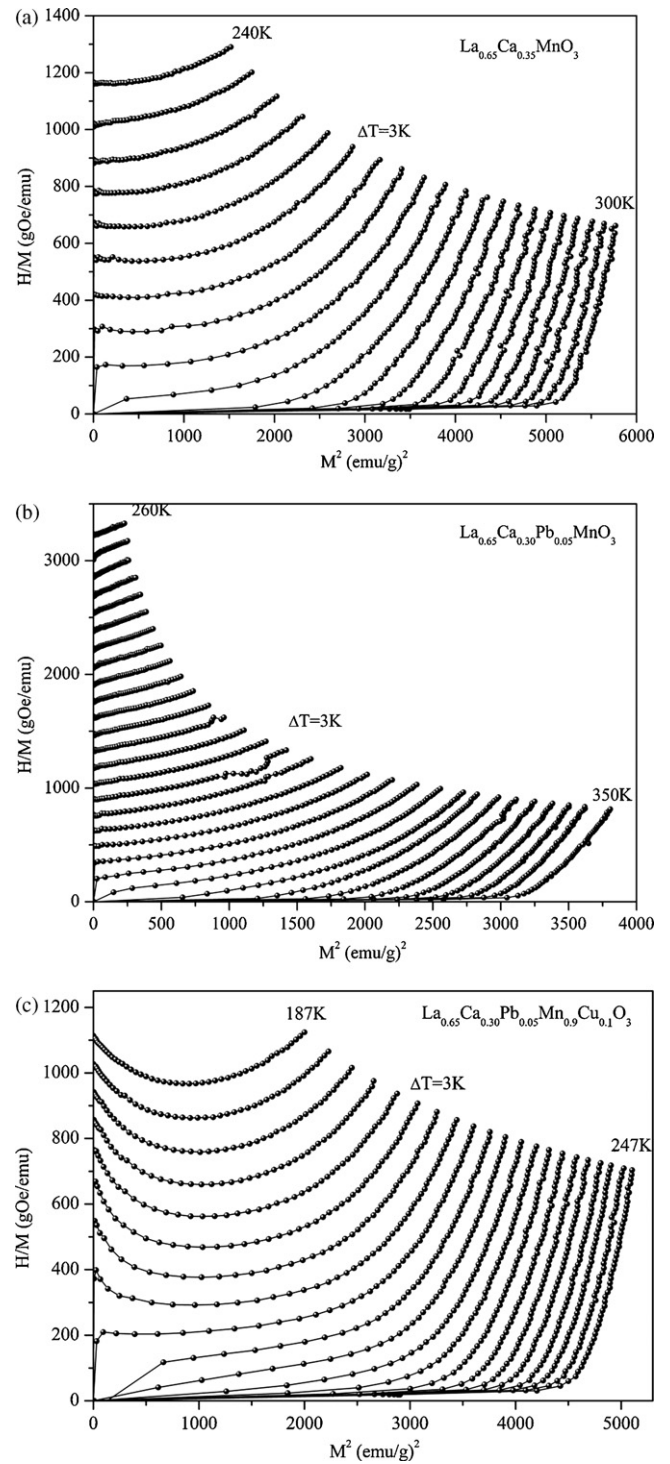


Fig. 5. H/M versus M^2 isotherms for the samples: (a) $\text{La}_{0.65}\text{Ca}_{0.35}\text{MnO}_3$, (b) $\text{La}_{0.65}\text{Ca}_{0.30}\text{Pb}_{0.05}\text{MnO}_3$, (c) $\text{La}_{0.65}\text{Ca}_{0.30}\text{Pb}_{0.05}\text{Mn}_{0.90}\text{Cu}_{0.10}\text{O}_3$.

ionic balance of the compound can be represented as $\text{La}_{0.65}^{3+}\text{Ca}_{0.30}^{2+}\text{Pb}_{0.05}^{2+}\text{Mn}_{0.45}^{3+}\text{Mn}_{0.45}^{4+}\text{Cu}_{0.10}^{2+}\text{O}_3^{2-}$. In this case, the $\text{Mn}^{3+}/\text{Mn}^{4+}$ ratio is equal to 1. Due to an increase in the number of Mn^{4+} ions, antiferromagnetic superexchange interaction increases. On the other hand, if the oxidation state of the Cu ions is 3+, the ionic balance may be written as $\text{La}_{0.65}^{3+}\text{Ca}_{0.30}^{2+}\text{Pb}_{0.05}^{2+}\text{Mn}_{0.55}^{3+}\text{Mn}_{0.35}^{4+}\text{Cu}_{0.10}^{3+}\text{O}_3^{2-}$. In this situation, although the ratio of the $\text{Mn}^{3+}/\text{Mn}^{4+}$ ions increases to 1.571, the average ionic radius of the B-site, (r_B), decreases; since the Cu^{3+} ions are smaller than the Cu^{2+} ions. It should

Table 2Comparison of T_C (K) and $|\Delta S_M|$ values, obtained in this work and from the literature under different preparation conditions.

Compound	T_C (K)	$ \Delta S_M $ (J/kg K)	H (T)	Preparation tech.	Sintering tem. ($^{\circ}$ C)	Ref.
$\text{La}_{0.65}\text{Ca}_{0.35}\text{MnO}_3$	273	4.1	1	Sol-gel	1100	Present
$\text{La}_{0.65}\text{Ca}_{0.35}\text{MnO}_3$	267.9	5.005	1.5	Sol-gel	1200	[24]
$\text{La}_{0.65}\text{Ca}_{0.35}\text{MnO}_3$	260	6.5	4	Solid-state	1350	[26]
$\text{La}_{0.67}\text{Ca}_{0.33}\text{MnO}_3$	256	4.3	1.5	Sol-gel	1200	[27]
$\text{La}_{0.67}\text{Ca}_{0.33}\text{MnO}_3$	268	6.9	2	Sol-gel	1250	[28]
$\text{La}_{0.67}\text{Ca}_{0.33}\text{MnO}_3$	269	6.1	3	Solid-state	1350	[29]
$\text{La}_{0.67}\text{Ca}_{0.33}\text{MnO}_3$	266	2.23	1	Sol-gel	1000	[30]
$\text{La}_{0.67}\text{Ca}_{0.33}\text{MnO}_3$	267	0.84	1	Sol-gel	1200	[31]

be noted that, the ionic radius of the Mn^{3+} and Cu^{3+} ions are nearly the same, and the ionic radius of the Cu^{2+} (0.73 Å) ion is bigger than that of Cu^{+3} (0.53 Å). If the oxidation state of copper ions entering into the structure is taken to be a mixture of 2+ and 3+, then the ionic balance of the compound can be written as $\text{La}_{0.65}^{3+}\text{Ca}_{0.30}^{2+}\text{Pb}_{0.05}^{2+}\text{Mn}_{0.55-0.1(1-a)}^{3+}\text{Mn}_{0.35+0.1(1-a)}^{4+}\text{Cu}_{0.1(1-a)}^{2+}\text{Cu}_{0.1a}^{3+}\text{O}_3^{2-}$ where “ a ” is the content of the Cu^{3+} ions in the compound. The content of the Mn^{4+} ions, depending on the content of Cu^{2+} can be written as $0.35 + 0.1(1 - a)$. If the $\text{Mn}^{3+}/\text{Mn}^{4+}$ content changes in between 0.35 and 0.45, then the $\text{Mn}^{3+}/\text{Mn}^{4+}$ ratio will vary between 1 and 1.571. Thus, $\langle r_B \rangle$ decreases while $\langle r_A \rangle$ remains the same. The variation in $\langle r_B \rangle$ gives rise to changes in Mn–O bond length and Mn–O–Mn bond angle. The ferromagnetic double exchange interaction diverges to antiferromagnetic superexchange interaction with decreasing $\langle r_B \rangle$. In this study, the decrease in T_C as a result of Cu substitution in B-site is an indication of a disorder caused by Cu atoms that reduces double exchange interaction, which in turn becomes less effective than antiferromagnetic superexchange.

The magnetization curves, $M(H)$, at temperatures separated by 3 K for the three samples below and above their Curie temperatures with respect to the external applied magnetic fields between 0 and 5 T, are given in Fig. 2a–c. It is seen that the field dependences of the magnetizations around the respective Curie temperatures are strong enough to generate high entropy changes even at low fields.

The saturation magnetization curves of the samples (taken at 5 K) for the applied fields up to 5 T are shown in Fig. 3. The saturations take place at very low magnetic fields (above 0.3 T). The saturation magnetization is known to be related to the maximum magnetic entropy change. In this study, the $\text{La}_{0.65}\text{Ca}_{0.35}\text{MnO}_3$ sample has given the greatest maximum magnetic entropy change value among the samples and this sample has also the highest saturation magnetization value, as seen in Fig. 3.

Isothermal magnetization measurements allow calculating the total magnetic entropy change, ΔS_M , of a sample through the following relation:

$$\Delta S_M(T, H) = \int_0^H \left(\frac{\partial M}{\partial T} \right)_H dH \quad (1)$$

However, in practice, an approximate magnetic entropy change value can be obtained from $M(H)$ curves by approximating the integration to a summation over discrete magnetization values at discrete temperatures and applied fields as the following:

$$(\Delta S_M)_i = \sum_j \frac{M(T_{i+1}, H_j) - M(T_i, H_j)}{T_{i+1} - T_i} (H_{j+1} - H_j) \quad (2)$$

where M_i and M_{i+1} are the experimental values of the magnetizations obtained at the temperatures T_i and T_{i+1} under the magnetic field H_j .

The temperature dependence of the magnetic entropies ($|\Delta S_M|$) determined at applied magnetic fields in between 1 and 5 T, for the our samples, are plotted in Fig. 4a–c. It is seen that the maximum magnetic entropy changes of the samples exhibit

a linear dependence on the magnetic field. Especially, the maximum magnetic entropy change of the $\text{La}_{0.65}\text{Ca}_{0.35}\text{MnO}_3$ compound is higher than that of the other samples. As can be seen from the figures the maximum magnetic entropy changes, for the field change from 0 to 1 T, are 4.1, 2.6, and 3.2 J/kg K for the $\text{La}_{0.65}\text{Ca}_{0.35}\text{MnO}_3$, $\text{La}_{0.65}\text{Ca}_{0.30}\text{Pb}_{0.05}\text{MnO}_3$ and $\text{La}_{0.65}\text{Ca}_{0.30}\text{Pb}_{0.05}\text{Mn}_{0.90}\text{Cu}_{0.10}\text{O}_3$ compounds, respectively. The $|\Delta S_M^{\max}|$ value decreases for the Pb-doped sample and increases for the Cu-doped sample. The maximum magnetic entropy change value of the $\text{La}_{0.65}\text{Ca}_{0.35}\text{MnO}_3$ sample obtained in this study is higher than most of the values published in the literature for the same compound (see Table 2).

It is well known that the ferromagnetic double exchange interactions between Mn^{3+} and Mn^{4+} ions is responsible for the large magnetic entropy change in manganese based compounds.

According to double exchange theory, shorter Mn–O bond distance and Mn–O–Mn bond angles closer to 180° strengthen the ferromagnetic interaction. Even though $\text{Mn}^{3+}/\text{Mn}^{4+}$ ratio is the same for the $\text{La}_{0.65}\text{Ca}_{0.35}\text{MnO}_3$ and $\text{La}_{0.65}\text{Ca}_{0.30}\text{Pb}_{0.05}\text{MnO}_3$ samples, the maximum magnetic entropy change value is lower for the $\text{La}_{0.65}\text{Ca}_{0.30}\text{Pb}_{0.05}\text{MnO}_3$ sample. This might be due to the increase in $\langle r_A \rangle$ as a result of Pb-doping in A-site, consequently, Mn–O bond distance and the Mn–O–Mn bond angle are expected to change.

The maximum magnetic entropy change of the $\text{La}_{0.65}\text{Ca}_{0.30}\text{Pb}_{0.05}\text{Mn}_{0.90}\text{Cu}_{0.10}\text{O}_3$ compound is higher than that of the $\text{La}_{0.65}\text{Ca}_{0.30}\text{Pb}_{0.05}\text{MnO}_3$ and lower than that of the $\text{La}_{0.65}\text{Ca}_{0.35}\text{MnO}_3$ compounds. The strength of ferromagnetic double exchange or the antiferromagnetic superexchange interactions depends on the valancy of the Cu ions for the $\text{La}_{0.65}\text{Ca}_{0.30}\text{Pb}_{0.05}\text{Mn}_{0.90}\text{Cu}_{0.10}\text{O}_3$ sample, since both the $\text{Mn}^{3+}/\text{Mn}^{4+}$ ratio and $\langle r_B \rangle$ would differ by the valancy of the Cu ions. Additionally, the ionic radii of the Cu^{2+} and the Cu^{3+} ions are different from each other and this difference causes the magnetic properties of the samples to be different.

A set of H/M versus M^2 curves for the $\text{La}_{0.65}\text{Ca}_{0.35}\text{MnO}_3$, $\text{La}_{0.65}\text{Ca}_{0.30}\text{Pb}_{0.05}\text{MnO}_3$ and $\text{La}_{0.65}\text{Ca}_{0.30}\text{Pb}_{0.05}\text{Mn}_{0.90}\text{Cu}_{0.10}\text{O}_3$ compounds are shown in Fig. 5. Positive slopes in a relatively small M^2 region above T_C indicate that all of the samples have second-order ferromagnetic to paramagnetic phase transition.

4. Conclusions

The magnetic and the magnetocaloric properties of the $\text{La}_{0.65}\text{Ca}_{0.35}\text{MnO}_3$, $\text{La}_{0.65}\text{Ca}_{0.30}\text{Pb}_{0.05}\text{MnO}_3$ and $\text{La}_{0.65}\text{Ca}_{0.30}\text{Pb}_{0.05}\text{Mn}_{0.90}\text{Cu}_{0.10}\text{O}_3$ manganite compounds have been investigated. The highest *para*-ferromagnetic phase transition temperature has been observed at 286 K for the $\text{La}_{0.65}\text{Ca}_{0.30}\text{Pb}_{0.05}\text{MnO}_3$ sample. On the contrary, the highest maximum magnetic entropy change value (for 0–1 T field change) has been found to be 4.1 J/kg K for the sample $\text{La}_{0.65}\text{Ca}_{0.35}\text{MnO}_3$. The substitution of Pb for Ca raise the transition temperature to 286 K. On the other hand, T_C tends to decrease while maximum magnetic entropy change increases with the Cu doping to the $\text{La}_{0.65}\text{Ca}_{0.35}\text{MnO}_3$ compound.

Acknowledgments

The authors would like to thank to Professor Mehmet Acet of Duisburg University for his contributions to the magnetic measurements and Professor Kerim Kiyamac for help in language corrections.

References

- [1] V.K. Pecharsky, K.A. Gschneidner Jr., *Phys. Rev. Lett.* 78 (1997) 4494.
- [2] V.K. Pecharsky, K.A. Gschneidner Jr., *J. Alloys Compd.* 260 (1997) 98.
- [3] V.K. Pecharsky, K.A. Gschneidner Jr., *Appl. Phys. Lett.* 70 (1997) 3299.
- [4] C. Ritter, et al., *J. Phys.: Condens. Matter* 18 (16) (2006) 3937–3950.
- [5] E. Bruck, *J. Phys. D: Appl. Phys.* 38 (2005) R381.
- [6] V.K. Pecharsky, K.A. Gschneidner Jr., *Adv. Cryog. Eng.* 43 (1998) 1729.
- [7] K.A. Gschneidner, V.K. Pecharsky, C.B. Zimm, *Mater. Technol.* 12 (1997) 145–149.
- [8] S. Kevran, Y. Elerman, M. Acet, *J. Alloys Compd.* 321 (2001) 35–39.
- [9] S. Kevran, M. Acet, Y. Elerman, *Solid State Commun.* 119 (2001) 95–99.
- [10] N.T. Hien, N.P. Thuy, *Physica B* 319 (2002) 168–173.
- [11] S. Fujieda, A. Fujita, K. Fukamichi, *Appl. Phys. Lett.* 81 (2002) 1276.
- [12] X. Hu, B.G. Shen, J.R. Sun, G.H. Wu, *Phys. Rev. B* 64 (2001) 132412.
- [13] C. Ritter, C. Magen, L. Morellon, P.A. Algarabel, M.R. Ibarra, V.K. Pecharsky, A.O. Tsokol, K.A. Gschneidner Jr., *J. Phys.: Condens. Matter* 18 (16) (2006) 3937–3950.
- [14] W. Cheikhrouhou-Koubaa, M. Koubaa, A. Cheikhrouhou, *J. Alloys Compd.* 453 (2008) 42–48.
- [15] M. Pekała, V. Drozd, *J. Alloys Compd.* 456 (2008) 30–33.
- [16] A.N. Ulyanov, J.S. Kim, G.M. Shin, Y.M. Kang, S.I. Yoo, *J. Phys. D: Appl. Phys.* 40 (2007) 123–126.
- [17] G.B. Chon, H.S. Im, S.M. Lee, B.H. Koo, C.G. Lee, M.H. Jung, *J. Magn. Magn. Mater.* 310 (2007) 927–929.
- [18] A. Pen, J. Gutierrez, J.M. Barandiaran, J.L. Pizarro, T. Rojo, L. Lezama, M. Insausti, *J. Magn. Magn. Mater.* 226–230 (2001) 831–833.
- [19] M.S. Reis, J.C.C. Freitas, M.T.D. Orlando, A.M. Gomes, A.L. Lima, I.S. Oliveira, A.P. Guimaraes, A.Y. Takeuchi, *J. Magn. Magn. Mater.* 242–245 (2002) 668–671.
- [20] O.I. Klyushnikov, V.V. Sal'nikov, N.M. Bogdanovich, *Inorg. Mater.* 38 (3) (2002) 261–264.
- [21] L. Pi, L. Zheng, Y. Zhang, *Phys. Rev. B* 61 (13) (2000).
- [22] H.D. Zhou, G. Li, X.Y. Xu, S.J. Feng, Y. Qian, X.G. Li, *Mater. Chem. Phys.* 75 (2002) 140–143.
- [23] M. Koubaa, W. Cheikhrouhou-Koubaa, A. Cheikhrouhou, A.-M. Haghiri-Gosnet, *Physica B* 403 (2008) 2477–2483.
- [24] J.-Q. Zhang, N. Li, M. Feng, B.-C. Pan, H.-B. Li, *J. Alloys Compd.* 467 (2009) 88–90.
- [25] M. Bejar, E. Dhahri, E.K. Hliil, S. Heniti, *J. Alloys Compd.* 440 (2007) 36–42.
- [26] R. Szymczak, M. Czepelak, R. Kolano, A.K. Burian, B. Krzymanska, H. Szymczak, *J. Mater. Sci.* 43 (2008) 1734–1739.
- [27] H. Huang, Z.B. Guo, D.H. Wang, Y.W. Du, *J. Magn. Magn. Mater.* 173 (1997) 302–304.
- [28] G.C. Lin, Q. Wei, J.X. Zhang, *J. Magn. Magn. Mater.* 300 (2006) 392–396.
- [29] V.S. Kolat, H. Gencer, M. Gunes, S. Atalay, *Mater. Sci. Eng. B* 140 (2007) 212–217.
- [30] W. Chen, L.Y. Nie, X. Zhao, W. Zhong, G.D. Tang, A.J. Li, J.J. Hu, Y. Tian, *Solid State Commun.* 138 (2006) 165–168.
- [31] D.L. Hou, Y. Bai, J. Xu, G.D. Tang, X.F. Nie, *J. Alloys Compd.* 384 (2004) 62–66.